Journal of Cellular Biochemistry 26:231–246 (1984)
Membrane Receptors and Cellular Regulation 71–86

Acidification of Endocytic Compartments and the Intracellular Pathways of Ligands and Receptors

Darrell J. Yamashiro and Frederick R. Maxfield

Department of Pharmacology, New York University School of Medicine, New York, New York 10016

Several hormones, serum proteins, toxins, and viruses are brought into the cell by receptor-mediated endocytosis. Initially, many of these molecules and particles are internalized into a common endocytic compartment via the clathrin-coated pit pathway. Subsequently, the ligands and receptors are routed to several destinations, including lysosomes, the cytosol, or the plasma membrane. We have examined the mechanism by which sorting of internalized molecules occurs. A key step in the process is the rapid acidification of endocytic vesicles to a pH of 5.0–5.5 This acidification allows dissociation of several ligands from their receptors, the release of iron from transferrin, and the penetration of diptheria toxin and some viral nucleocapsids into the cytoplasm. Transferrin, a ligand that cycles through the cell with its receptor, has been used as a marker for the recycling receptor pathway. We have found that in Chinese hamster ovary (CHO) cells transferrin is rapidly segregated from other ligands and is routed to a complex of small vesicles and/or tubules near the Golgi apparatus. The pH of the transferrin-containing compartment is approximately 6.4, indicating that it is not in continuity with the more acidic endocytic vesicles which contain ligands destined to be degraded in lysosomes.

Key words: endocytosis, transferrin, receptors, endocytic vesicles

Receptor-mediated endocytosis is important in a wide range of biological functions. Proteins such as asialoglycoproteins [1] and α_2-macroglobulin-endoprotease complexes [2,3] are cleared from serum by receptor-mediated endocytosis and are degraded in lysosomes. The cholesterol carrier low-density lipoprotein (LDL) is also internalized, and in this case degradation allows free cholesterol to be released to the cell [4]. Lysosomal enzymes bind to cell surface receptors and are delivered to lysosomes [5,6]. Transferrin releases its bound iron following endocytosis, and the apotransferrin recycles back to the cell surface [7,8]. Several hormones and growth factors are internalized after binding to their receptors [3]. A variety of toxins, such as diptheria toxin and ricin toxin [9,10], and viruses, such as Semliki Forest virus [11], take advantage of the endocytic pathway and penetrate into the cell cytosol from a nonlysosomal compartment.

Received July 18, 1984, accepted August 27, 1984.

It is therefore clear that ligands that are internalized through a common process can have markedly different destinations. Not only is this the case for the ligands, but receptors can follow paths that are separate from their respective ligands. For example, the receptors for α_2-macroglobulin (α_2M) [12,13], asialoglycoproteins [14,15], and LDL [16] are not degraded, but recycle to the cell surface and escape the fate of their ligand. In this manner, receptors can be used in multiple rounds of endocytosis, giving the cell a highly efficient mechanism for internalizing vast quantities of ligand [17].

This review will discuss the work conducted in our laboratory to determine how ligands and receptors are directed to different locations. In particular, we will focus on the intracellcular pathways of α_2M and transferrin in Chinese hamster ovary (CHO) cells [18]. Both ligands bind to specific receptors on cell surfaces and are rapidly internalized. However, their fates after internalization are markedly different. α_2M is delivered to lysosomes for degradation [18–20], whereas transferrin is recycled back to the cell surface [18,21–24]. By comparing the recycling pathway of transferrin with the well-characterized degradative pathway of α_2M, we have been able to identify the structures involved in recycling transferrin and its receptor back to the cell surface [18].

MATERIALS AND METHODS

Microspectrofluorometric Measurement of the pH of Endocytic Compartments

Measurements of the pH of endocytic compartments are based on the pH-dependent excitation profile of fluorescein-labeled macromolecules. Fluorescence intensity measurements are made at two excitation wavelengths (e.g., 450 nm and 490 nm). The ratio of intensities (I_{450}/I_{490}) is strongly pH-dependent between pH 5 and pH 7 (Fig. 1). Cells were incubated with fluorescein-labeled macromolecules under conditions which deliver the macromolecule to a particular endocytic compartment, and fluorescence intensity measurements are made (see below). The I_{450}/I_{490} intensity ratio for fluorescein in the endocytic compartment is compared to I_{450}/I_{490} ratio values obtained from a series of pH-buffered solutions, and the pH of the endocytic compartment is obtained. The principle of the pH measurements is relatively simple, but a number of technical problems arise owing to the weak fluorescence signal from the relatively small number of molecules internalized by a cell. Reviews describing microspectrofluorometric measurement of pH have been published [25,26]. Here we describe methods we have used to measure the pH of specific endocytic compartments either by single-cell intensity measurements or by digital analysis of video images.

Single-cell intensity measurements have been made using a Leitz MPV microscope spectrofluorometer system modified to allow simultaneous video observations and measurement. There are several features of the system that have proved necessary for measuring intensities of single cells. The illumination and measurement fields are adjustable and can be aligned precisely. This results in a large reduction in the effects of stray light. Electronically controlled shutters limit the exposure time to approximately 0.1 sec per measurement, effectively eliminating effects of photobleaching. An image intensifier video camera can be used to center and focus cells in the

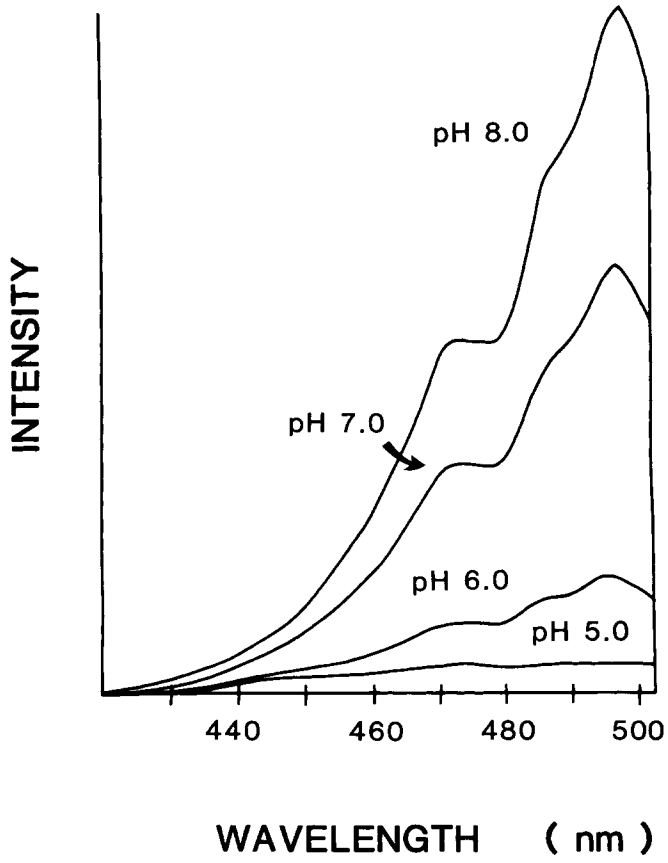

Fig. 1. pH dependence of fluorescein fluorescence. α_2-Macroglobulin was labeled using fluorescein isothiocyanate, and the labeled protein was dissolved in buffers at the indicated pH values. Fluorescence excitation profiles were obtained, with the emisson wavelength held fixed at 520 nm. As shown in the figure, the excitation of fluorescein fluorescence is strongly pH-dependent between pH 5 and pH 8.

measurement field and to observe fluorescence patterns at the time of measurement. Intensity measurements are made at 525-nm emission with either 450-nm or 490-nm narrow bandpass excitation filters.

A significant problem in quantitative fluorescence microscopy is intrinsic fluorescence (autofluorescence) of the cells. In many experiments the autofluorescence is comparable in magnitude to the fluorescein fluorescence intensity. When the autofluorescence is uniform within a culture, intensity measurements can be made from several untreated cells, and the average value is then subtracted from measurements on cells incubated with fluorescent macromolecules. Sometimes autofluorescence is very variable from cell to cell. In these cases, it is necessary to measure the autofluorescence of a single cell, expose the cell to a fluorescent ligand on the microscope stage, rinse away unbound fluorescence, and measure the fluorescence intensity of the same cell. This procedure allows accurate determination of fluorescein fluorescence even in highly autofluorescent cells [27].

Digital Image Analysis

Digital analysis of video images provides a significant advantage over whole-cell intensity measurements in certain circumstances. With an image intensifier video camera, images can be obtained at high magnification, yielding several thousand intensity measurements per cell. This allows us to make simultaneous pH measurements on individual endocytic compartments in a single cell [18,27]. Also, when the autofluorescence is evenly distributed while the fluorescein fluorescence is punctate, we can subtract out the autofluorescence before making pH measurements [18,27].

Image Digitization and Processing

Video images were obtained using either a DAGE/MTI 65 MKII camera or a Zeiss-Venus TV3M camera, and recorded using a Panasonic NV8030 video tape recorder. Images were digitized into a 484 × 512 matrix of picture elements ("pixels"), with 256 intensity levels per pixel, using a CAT800 Image Digitizer (Digital Graphics, Palo Alto, CA) housed in a Northstar 64K microcomputer. To improve the signal-to-noise ratio for digitized images, the pixel intensities of four to eight video frames were averaged. The digitized images were transmitted to a MINC 11/23 (Digital Equipment Corp) for further processing. A locally defined background fluorescence was defined as the 50th percentile (ie, median) intensity in either a 32 × 32 pixel segment (ca 6.5 × 6.5 μm) for experiments with F-α_2M and fluorescein-labeled asialo-orosomucoid (ASOR) or a 32 × 64 pixel segment (6.5 × 13 μm) for experiments with fluorescein-transferrin (F-Tf). This background value was subtracted from all pixel intensities. A threshold intensity value was then chosen such that the pixel intensities used to calculate the I_{450}/I_{490} ratio would be derived from bright areas corresponding to endocytic compartments.

The validity of the image processing method was tested by varying the background and threshold values. Within a reasonable range for these parameters, only small changes ($\sim$0.2 pH units) were obtained [27]. In addition, we have constructed a pH calibration curve for each set of experiments. For example, CHO cells were incubated with fluorescein-labeled ligand under the same conditions used during the actual experiments. The cells were fixed with 2% formaldehyde in PBS containing 1 mM $CaCl_2$ for 10 min. Cells were then rinsed in PBS and placed in solutions of pH 5.0, 6.0, and 7.0. The solutions contained 150 mM NaCl, 5 mM KCl, 1 mM $CaCl_2$, and 10mM glucose, and were buffered as follows: pH 5.0 with 50 mM Tris-maleate; pH 6.0 with 25 mM Tris-maleate and 25 mM sodium phosphate; and pH 7.0 with 50 mM sodium phosphate. Monensin (40 μM) was added to dissipate any pH gradients. Fluorescence images at 450-nm and 490-nm were recorded and processed as described above.

RESULTS AND DISCUSSION

Internalization of Ligands and Receptors by a Shared Pathway

In 1976 Anderson, Goldstein, and Brown demonstrated that receptors for low-density lipoproteins (LDL) clustered over clathrin-coated regions of the plasma membrane and that endocytic vesicles containing LDL formed from these coated pits [28]. Since then, a number of workers have shown that several ligands, including hormones, serum proteins, and viruses, enter cells via receptor-mediated endocytosis. Initially these ligands appear to enter the cell through a shared pathway. Double-

labeling experiments using light and electron microscopy have shown that many of these ligands are found mixed together in the same endocytic vesicle [3,29]. Several receptors which are internalized along with their ligands return to the cell surface and are reutilized. Many of the ligands are degraded, but some (eg, diphtheria toxin [30,31] and the nucleocapsids of some viruses [32]) enter the cytoplasm.

Acidification of Endocytic Vesicles

There was reason to suspect that exposure to an acid pH was involved in the sorting of ligands and receptors within the cell. Weak bases, which raise the pH of acidic organelles [33–35], could protect cells against diptheria toxin and enveloped viruses [11,30,31]. Weak bases also caused a depletion of cell surface receptors for lysosomal enzymes [36,37], apparently by blocking receptor reutilization. Furthermore, exposure to a low pH could cause penetration into the cytoplasm of membrane-bound diptheria toxin [30,31] or Semliki Forest virus [32], and several ligands were shown to dissociate from their receptors at low pH [36–38]. Ben Tycko and one of us (F.R.M.) sought to determine the kinetics of exposure of endocytosed ligands to acid pH. We expected that this might correlate with the entry of ligands into lysosomes, since those were thought to be the only acidic organelles along the endocytic pathway. Using microspectrofluorometric pH measurements with fluorescein-labeled-α_2-macroglobulin (F-α_2M), it was found [39] that endocytic vesicles in mouse fibroblasts are acidified to a pH of 5.0 rapidly after internalization (ie, within 5–15 min). This result was surprising initially because it had been shown that α_2M does not reach lysosomes in mouse fibroblasts for at least 20 min. Using several methods, including electron-microscopic cytochemistry, it was confirmed that the initial acidic vesicle along the endocytic pathway was not a lysosome [39]. Similar results have been obtained with asialoglycoprotein in human hepatoma cells [27].

Exposure to a low pH in a nonlysosomal compartment would allow dissociation of many ligands from their receptors [35] without exposure of the receptors to lysosomal enzymes. Similarly, viruses and diptheria toxin, which are rapidly inactiviated by degradative enzymes, could penetrate into the cytoplasm without exposure to lysosomes. One of the more interesting effects of exposure to low pH has been documented for the iron transport protein transferrin. This protein binds to cell surface receptors and is internalized by receptor-mediated endocytosis [21–24, 40–42]. When exposed to an acidic pH, transferrin releases its iron but remains bound to its receptor [22–24,43]. The receptor-bound apotransferrin returns to the cell surface where exposure to neutral pH causes dissociation of the apotransferrin from the transferrin receptor. Thus, transferrin is a ligand that follows a pathway through the cell analogous to the pathway of recycling receptors. We [18] and others [42,44] have compared the intracellular fate of transferrin, which is a marker for the recycling pathway, with other ligands that are degraded in lysosomes. These studies are providing new information about the sorting of ligands and receptors within the cell. Our studies have focused on the fate of transferrin and α_2-macroglobulin in CHO cells.

Initial Entry Into Cells

Transferrin and α_2M bind to specific cell surface receptors and are internalized [19,20,45,46] through clathrin-coated pits [40,41,47–49]. The first intracellular compartment we can identifiy in CHO cells by electron microscopy is a class of small

vesicles and tubular structures of diameter less than 120 nm (Fig. 2). In quantitative electron microscopy with colloidal gold α_2M (α_2M-gold), we have found that 48% of the α_2M-gold is found in these structures [18] after a 5-min uptake at 37°C. At later times, over 80% of the α_2M-gold was found in large vesicles and multivesicular bodies (diameters > 120 nm). This suggests that α_2M transiently passes through small vesicles and tubular structures before entering the larger vesicles.

We obtained similar results at early times when we examined the pathway of transferrin conjugated with ferritin (Tf-Fer). With a 5-min continuous uptake at 37°C, the majority of Tf-Fer (79%) was found in small vesicles and tubules. These results suggest that the first intracellular compartment for both transferrin and α_2M is small vesicles and tubules. We cannot strictly rule out the possibility that larger endocytic vesicles are the first intracellular compartment, but our data are most consistent with initial delivery to small vesicles and tubules.

Previous electron-microscopic studies support the concept that the first site after internalization may be small vesicles and tubular structures in the periphery of the cell. These types of structures have been shown to contain asialoglycoproteins in primary hepatocytes [50] and in a human hepatoma cell line [51]. Previous studies have also demonstrated that transferrin and its receptor are found at early times in small vesicles and tubular structures [40,52,53]. These peripheral endocytic compartments often consists of tubular elements which can form anastamosing networks.

Segregation of Transferrin From α_2M

Morphological evidence has suggested that the small vesicles and tubules fuse together to form the larger vesicles termed receptosomes [29], CURL (compartment of uncoupling receptor and ligand) [51], endosomes [54], or endocytic vesicles. Endocytic vesicles can be distinguished from lysosomes by histochemical staining; endocytic vesicles do not contain detectable acid phosphatase or aryl sulfatase activity.

Our morphologic studies with CHO cells demonstrate that the majority of α_2M rapidly accumulates in endocytic vesicles [18]. After a 10-min uptake, with a 5-min chase, 76% of the α_2M was found in large acid phosphatase–negative vesicles similar to those we have previously found with α_2M in mouse fibroblasts [39] and with asialoglycoproteins in human hepatoma cells [27].

In contrast, the majority of the transferrin remains in small vesicles or tubules (diameter < 120 nm). These small vesicles and tubules, which have transferrin, but not α_2M, may be considered to be on the recycling part of the endocytic pathway. Morphologic evidence has been obtained by Geuze et al [51,55] that suggests that endocytic vesicles are the site at which ligands segregate from their receptors. They suggest that the large vesicles acquire lysosomal enzymes. The tubular extensions pinch off and recycle back to the cell surface, carrying the receptor. By forming small-volume recycling vesicles it would be possible to exclude free ligand, which would remain with the bulk of the fluid in the larger vesicles.

Initial Characterization of the Recycling Pathway in CHO Cells

The degradative pathway which involves endocytic vesicles and lysosomes is well characterized both morphologically and biochemically. Little is known, however, about the structures involved in recycling receptors back to the cell surface. We have

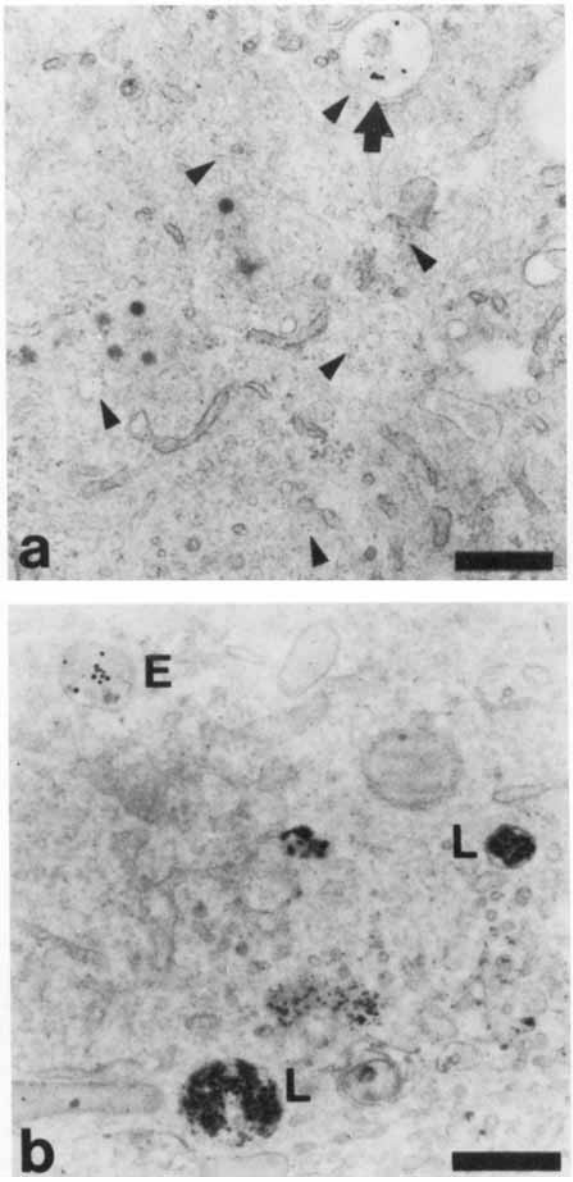

Fig. 2. Ultrastructural localization of α_2M-gold and Tf-Fer. CHO cells were incubated either (a) with Tf-Fer and α_2M-gold for 5 min, rinsed, and reincubated for 5 min; or (b) with only α_2M-gold for 10 min, rinsed, reincubated for 5 min, and then fixed and stained for acid phosphatase. Small arrowheads (a) indicate the location of some of the Tf-Fer particles in the micrograph. Tf-Fer and α_2M-gold (large arrow) can be found within the same endocytic vesicle, but the majority of Tf-Fer is found in small-diameter vesicles and tubules. The majority of α_2M-gold after a 10-min uptake and 5-min rinse (b) is found in large endocytic vesicles (E). However, at this time some α_2M-gold can be found in acid-phosphatase-positive lysosomes (L). Colloidal gold particles are easily seen over the background of acid phosphatase reaction product. Bar, 0.5 μm. [Reprinted from 18.]

examined the pathway followed by transferrin to characterize the recycling pathway in CHO cells. Receptor localization studies with antitransferrin antibodies [56], density gradient sedimentation [57], and a receptor solubilization assay [18] demonstrated that transferrin was in the same compartment as its receptor. At the light microscope level, F-Tf was found in CHO cells in a large, juxtanuclear structure with a diameter of approximately 3 μm. We did not at any time detect F-Tf in a punctate pattern.

The juxtanuclear distribution of F-Tf suggested that transferrin was routed to the Golgi complex. Since the Golgi complex contains a high concentration of clathrin [58], we conducted immunolocalization studies with anticlathrin antibodies [59,60]. Figure 3 demonstrates that the F-Tf containing structure (Fig. 3B) co-localized at the light-microscope level with the major site of intracellular clathrin (Fig. 3a). Wheat germ agglutinin (WGA) has a preferential affinity for the Golgi complex [61] and associated small vesicles and tubules [62]. In detergent-permeabilized cells R-WGA also colocalized with the F-Tf containing structure. These results suggest that the transferrin-containing structure is associated with the Golgi complex.

Studies at the electron microscope level confirmed the finding that transferrin associates with the Golgi complex as it recycles. Figure 4 illustrates that Tf-Fer accumulates in small vesicles and tubular structures adjacent to the Golgi complex. We did not detect ferritin particles in the Golgi stacks at any time. These results suggest that after the tubular extensions of endocytic vesicles pinch off they are routed to the para-Golgi region.

It is of interest that vesicles along the exocytic portion of the recycling pathway accumulate near the Golgi apparatus. In developing erthyroid cells, routing to the para-Golgi appears to directly correlate with the development of the Golgi complex [41]. The relationship, if any, between these exocytic recycling vesicles and the compartments responsible for routing of newly synthesized proteins to either the cell surface [63], or to lysosomes [5,6], remains to be determined.

Two Endocytic Compartments Maintain Different pH Values

Since the vesicles containing transferrin differed morphologically from endocytic vesicles containing α_2M, we wondered whether the pH of the transferrin-containing structure was similar to that of endocytic vesicles in the degradative pathway. To measure the pH of fluorescein-containing structures in CHO cells, we used image intensified video fluorescence microscopy and digital image analysis [18,27]. An advantage of digital image analysis techniques is that fluorescence intensity measurements can be easily corrected for cellular autofluorescence. Thus, we were able to measure exclusively the pH of the para-Golgi structure, excluding fluorescence contributed by either cell surface or internalized, peripheral F-Tf. Similarly, the punctate pattern of F-α_2M fluorescence was easily resolved against a diffuse background of autofluorescence.

The pH of F-Tf-containing structures is significantly different from that of the F-α_2M-containing structures [18]. We found that the average pH of the F-Tf-containing structures was 6.4, even after an uptake of only 5 min. Endocytic vesicles containing F-α_2M had an average pH of 5.4. These results demonstrate that transferrin rapidly enters a compartment that is significantly less acidic than endocytic vesicles. The electron microscopy data suggest that this mildly acidic pH is a characteristic of the small vesicles and tubules associated with the Golgi complex. The mildly acidic pH also emphasizes that the small vesicles and tubules are a

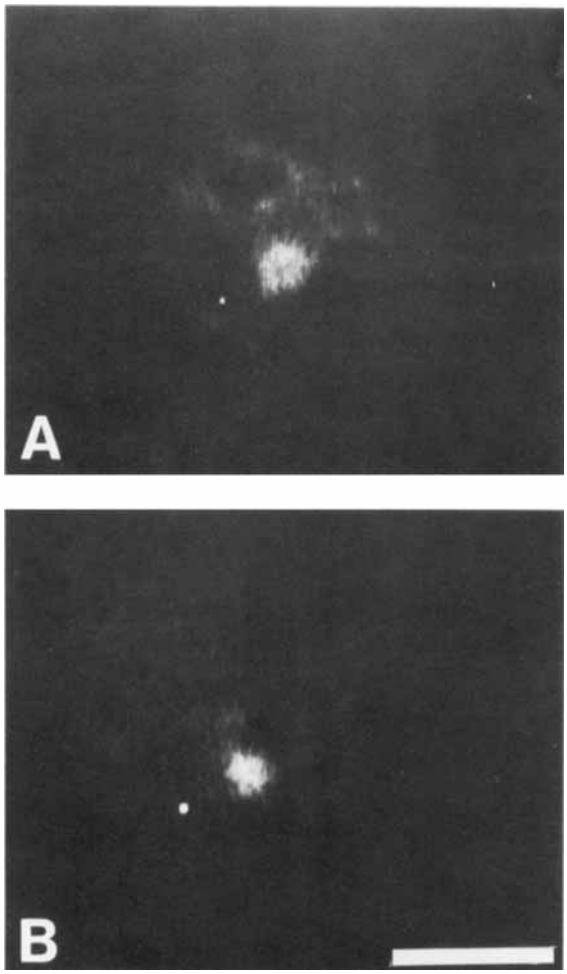

Fig. 3. Co-localization of F-Tf and rhodamine-labeled anticlathrin antibodies. CHO cells were incubated with F-Tf for 18 min and then rinsed for an additional 2 min. The cells were then fixed, permeabilized, and exposed to anticlathrin antibody (kindly provided by Dr James Keen, Fels Institute) and rhodamine-labeled second antibody. Rhodamine (A) and Fluorescein (B) fluorescence images were obtained and photographed. Bar, 8 μm.

compartment distinct from endocytic vesicles. Figure 5 shows images of cells incubated with F-Tf excited at 450 nm and 490 nm, before and after correction for background autofluorescence and application of a threshold intensity.

Oka and Weigel have reported that a significant percentage (as much as 50% under certain conditions) of internalized asialoglycoprotein enters a compartment where it remains bound to the receptor [64]. This would be expected if asialoglycoproteins remained in tubular structures with a pH above 6.0, similar to compartments that contain transferrin. Wall et al [50] have demonstrated morphologically the entry of asialoglycoproteins into such tubular structures. Similarly, some of the lysosomal enzymes that enter macrophages remain receptor-bound after internalization, whereas the majority of the ligands undergo a pH-induced dissociation from their receptor [36].

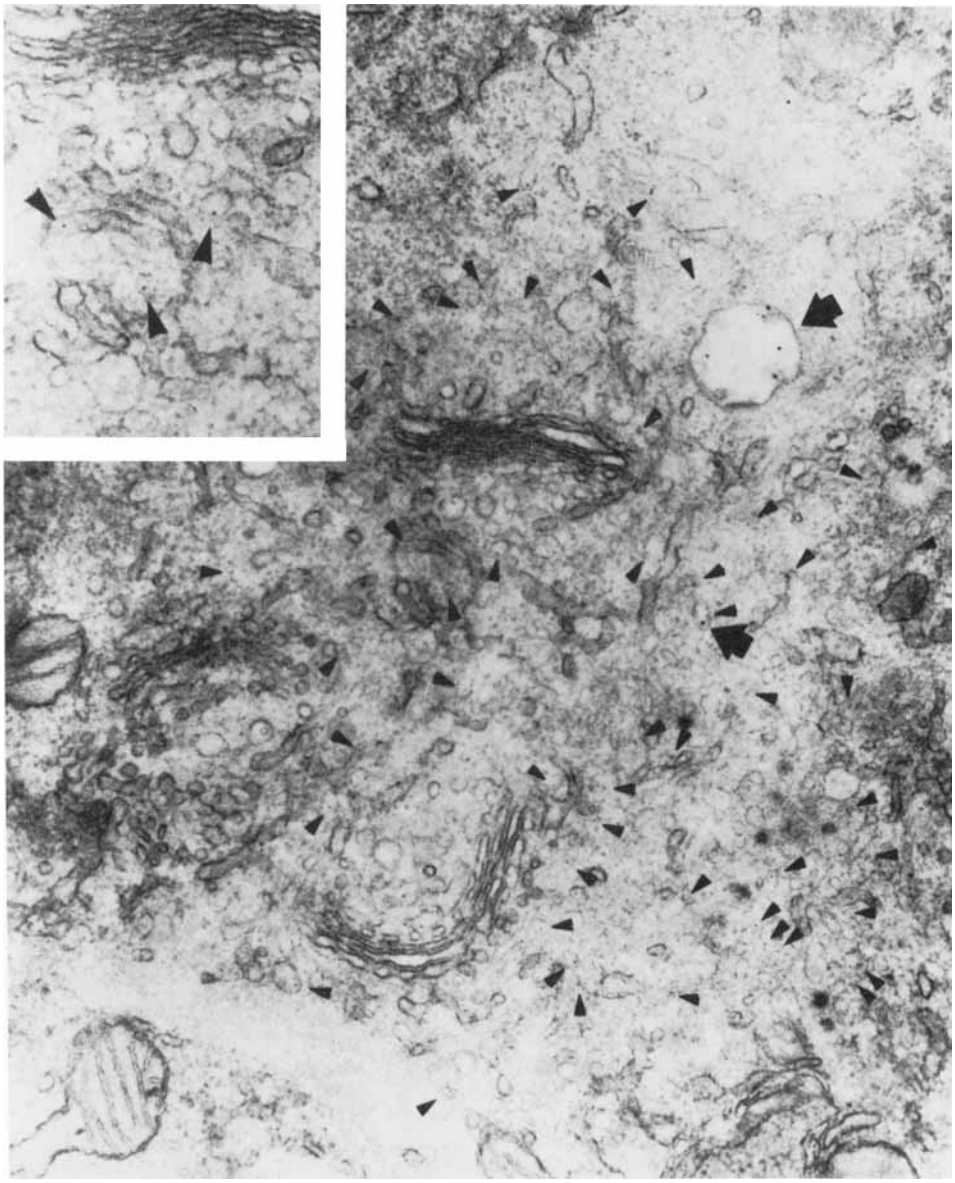

Fig. 4. TF-Fer is found near the Golgi complex. CHO cells were incubated with Tf-Fer and α_2M-gold for 10 min, rinsed, and reincubated for 5 min at 37°C. The vast majority of Tf-Fer (small arrow heads) is found in small-diameter vesicles and tubules near the Golgi complex. (Only some of the Tf-Fer particles are indicated by arrow-heads.) α_2M-Gold is found in a large endocytic vesicle (top large arrow) and also colocalizes (bottom large arrow) with Tf-Fer. The inset is an enlargement of the center portion of the micrograph, showing Tf-Fer in small-diameter vesicles and tubules just below the stacks of the Golgi complex. [Reprinted from 18.]

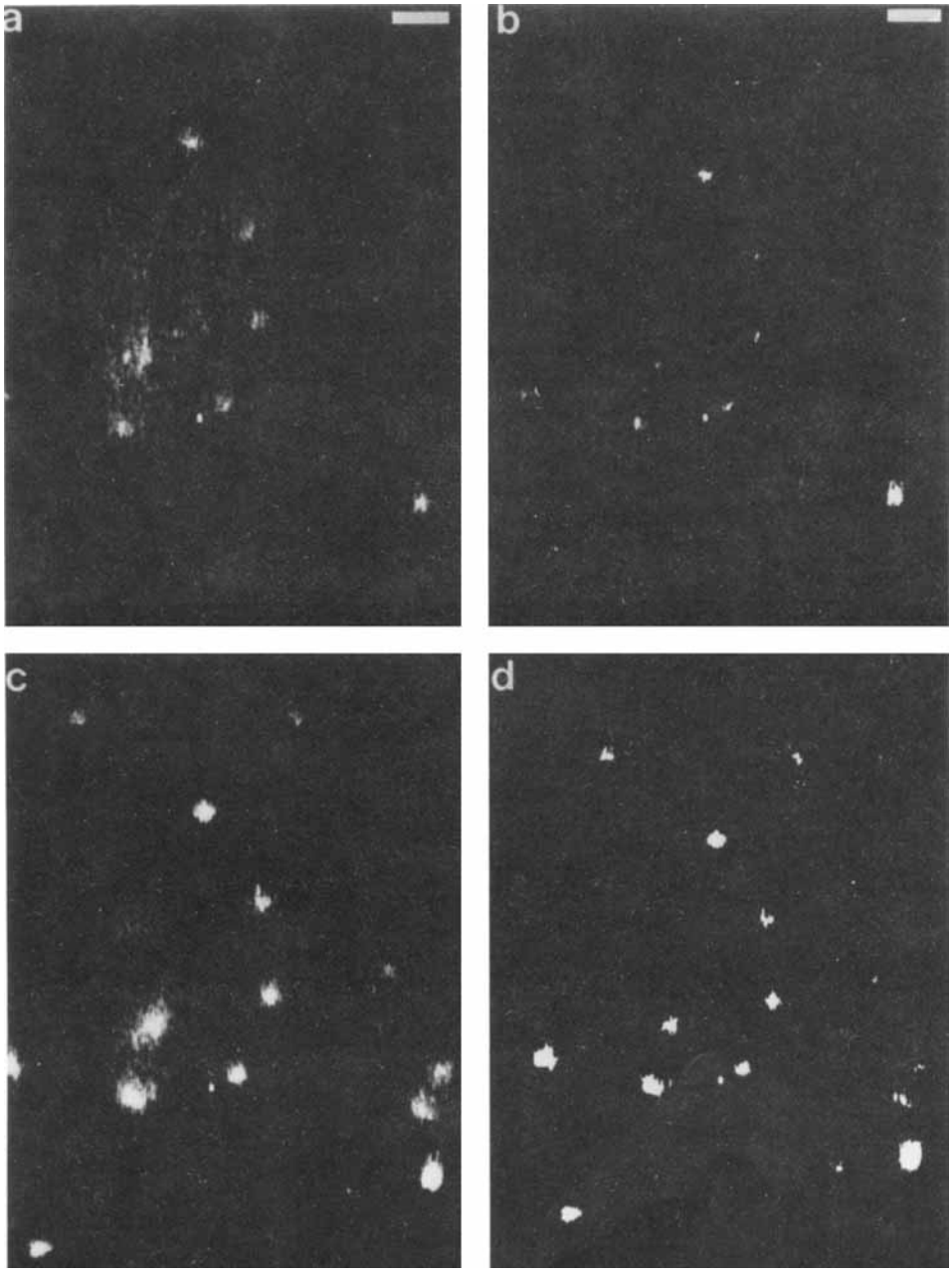

Fig. 5. Digitized and processed images of F-Tf-containing structures. CHO cells were incubated with F-Tf for 18 min at 34°C, and then rinsed free of unbound ligand for an additional 2 min. Fluorescence images were obtained and digitized as described in Methods. The images are: a) 450-nm excitation, digitized image; b) 450-nm excitation, digitized image corrected for background fluorescence and with threshold mask applied; c) 490-nm excitation: d) 490-nm excitation, digitized image corrected for background fluorescence and with a threshold intensity mask applied. Bar, 8 μm. [Reprinted from 18.]

The F-Tf-Containing Structure Actively Maintains Its Mildly Acidic pH

To determine if the F-Tf-containing structure actively maintains its acidic pH, we used the ionophore monensin to collapse the proton gradient [18,35]. To monitor the changes in pH, we measured the changes in the fluorescence intensity at 490-nm excitation using a microscope spectrophotometer. In intact cells, monensin rapidly dissipated the proton gradient of the F-Tf-containing structure, as indicated by the increase in the fluorescence intensity (Fig. 6). The reversibility of the effect of monensin in intact cells demonstrates that the F-Tf-containing structure, like endocytic vesicles [35], actively maintains its pH gradient.

Our results indicate that the vesicles that recycle back to the cell surface have lost the capacity to acidify to pH values below approximately 6.4. The simplest interpretation of this finding is that the majority of the endocytic vesicle proton pumps do not recycle along with transferrin to the surface; instead they remain with the vesicles that develop into lysosomes. It is possible, however, that some proton pumps recycle in the same compartments as receptors and transferrin, and that other factors regulate the pH to a higher value. The postsegregation recycling compartment can actively maintain a pH below that of the cytoplasm, and it is likely that it acidifies by an ATP-dependent mechanism as has been described for other compartments along the endocytic pathway.

Acidification of Compartments Along the Endocytic Pathway

ATP-dependent proton pumps have described for lysosomes [65–67], endocytic vesicles [68], pinosomes labeled with a fluid phase marker [69,70], purified clathrin-coated vesicles [71,72], and membranes from the Golgi [73]. These proton pumps appear to be insensitive to vanadate, suggesting that they do not require the formation of a phosphorylated intermediate in contrast to many cation-transporting ATPases [74–76].

However, there do seem to be differences among the various acidification mechanisms. Endocytic-vesicle acidification is less sensitive than lysosome acidification to the anion transport inhibitor DIDS (4,4′-diisothiocyanostilbene-2,2-disulfonic acid). In addition, the clathrin-coated vesicle proton pump is sensitive to the polypeptide antibiotic duramycin [78], which does not appear to inhibit either the lysosomal [77,78] or the endocytic-vesicle proton pump (Yamashiro and Maxfield, unpublished observations). It therefore appears that the endocytic vesicle and lysosomal acidification mechanisms are somewhat different from the clathrin-coated vesicle and Golgi membrane vesicle acidification mechanisms.

It is possible that the proton pumps for the various organelles are identicial, and that the differences lie with the associated cotransporters. The proton pumps may shuttle between various membranes of the cell. For example, Gluck et al [79] have shown that the acid-secreting cells of the turtle bladder have an intracellular pool of proton pumps which translocate to the luminal membrane upon stimulation with CO_2. The exact relationship between the acidification mechanisms of the various organelles remains to be defined by future work.

CONCLUSION

In Figure 7, we present a hypothetical model which illustrates our current understanding of the pathways taken by transferrin and α_2M following endocytosis

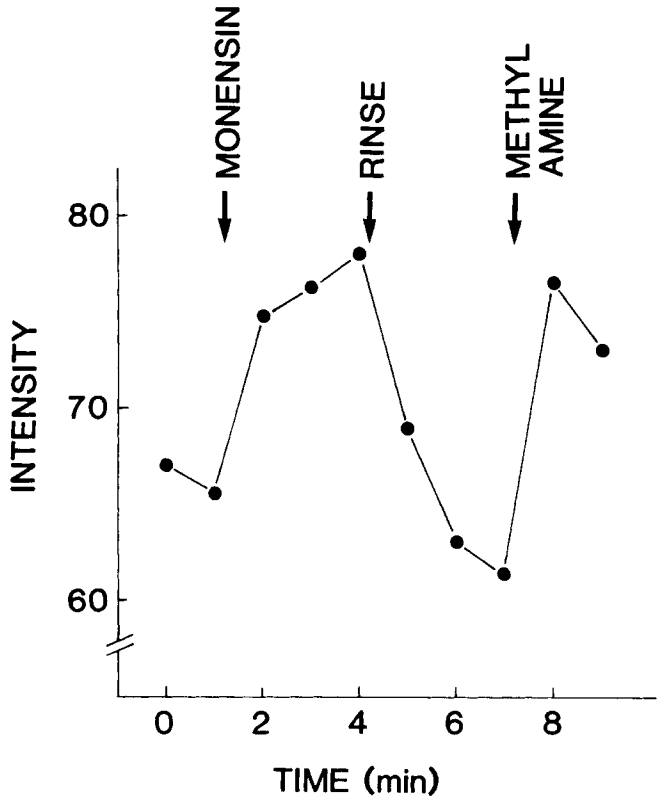

Fig. 6. Reversibility of the effect of monensin on the pH of fluorescein-transferrin (F-Tf)-containing structures. CHO cells were incubated with F-Tf (100 μg/ml in medium containing ovalbumin (1 mg/ml) for 18 min at 34°C and then rinsed free of unbound ligand for an additional 2 min. The cells were then placed on the microscope stage, and the fluorescence intensity of a group of six cells measured with 490-nm excitation using the microscope photometer (0 min). Monensin (10 μM) was added after 1 min, and the pH gradient was rapidly dissipated as indicated by the increase in fluorescence intensity. The cells were rinsed free of monensin at 4 min, and the F-Tf-containing structure rapidly reacidified as indicated by the decrease in the fluorescence intensity to approximately the initial value. The addition of methylamine (20 mM) at 7 min rapidly dissipated the pH gradient, confirming that the F-Tf-containing structure had reacidified.

by CHO cells. We wish to emphasize that this model illustrates a working hypothesis. Briefly, the model shows both ligands entering the cell via clathrin-coated pits which deliver the ligands and receptors to a peripheral compartment of small vesicles and tubules. Acidification to a pH of 5.0 to 5.5. occurs in a large tubulovesicular structure, causing dissociation of α_2M, but not transferrin, from its receptor. α_2M receptors and transferrin-receptor complexes remain in the tubular elements. The pH of the large vesicular structures remains at approximately 5.5, and these structures later acquire lysosomal enzymes. The tubular elements separate from the large vesicles, and their pH rises to approximately 6.4. Transferrin and receptors accumulate in small vesicles and tubular structures near the Golgi complex, and from this region they are transported back to the cell surface.

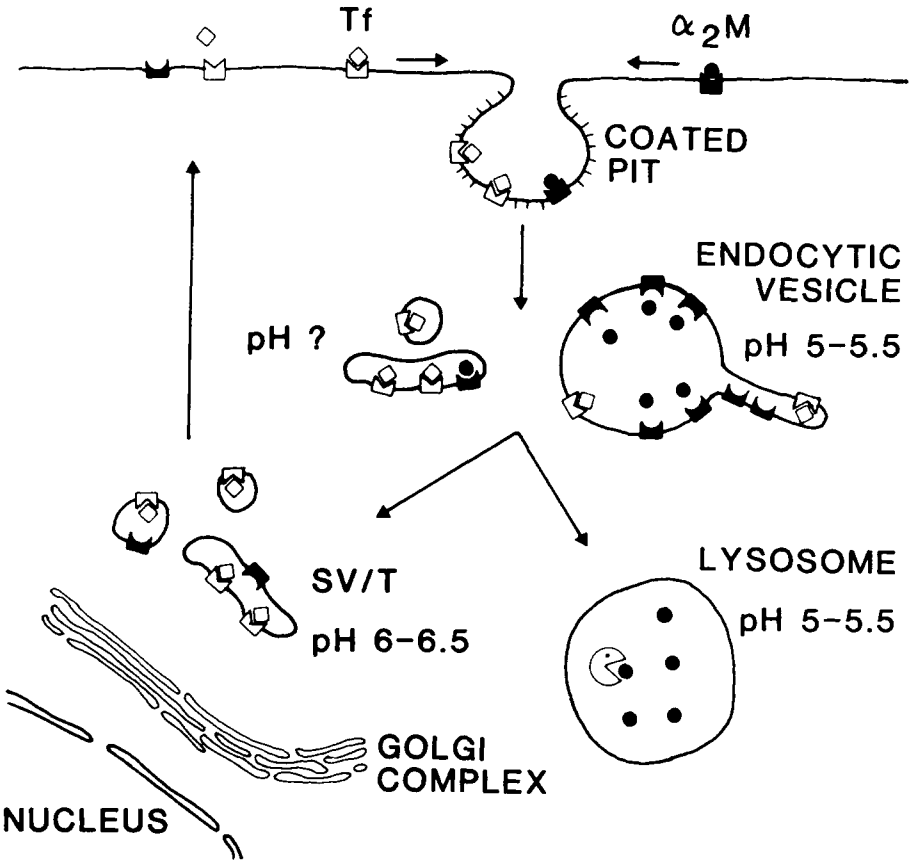

Fig. 7. Model of the endocytic pathways of transferrin and α_2M in CHO cells. Both transferrin and α_2M bind to specific receptors on the surface of cells and are internalized through clathrin-coated pits. The receptors for α_2M and the transferrin-receptor complex are routed to small vesicles and tubules (SV/T) near the Golgi complex, where they accumulate before returning to the cell surface. α_2M is delivered to lysosomes where it is degraded by lysosomal enzymes.

ACKNOWLEDGMENTS

This research was supported by grants from the NIH (AM 27083) and the Irma T. Hirschl Charitable Trust. We are grateful to Drs. B. Tycko, M.L. Shelanski, and C.H. Keith, and Mr. B.A. Kruskal for helpful discussions.

REFERENCES

1. Ashwell G, Harford J: Annu Rev Biochem 51:531, 1982.
2. Van Leuven F: Trends Biochem Sci 7:185, 1982.
3. Maxfield FR, Schlessinger J, Shechter Y, Pastan I, Willingham MC: Cell 14:805, 1978.
4. Brown MS, Kovanen PT, Goldstein JL: Science 212:628, 1981.
5. Neufeld EF: In Callahan JW, Lowden JA (eds): "Lysosomes and Lysosomal Storage Disease," New York: Raven Press, 1981, pp 115–129.

6. Sly WS, Fischer HD: J Cell Biochem 18:67, 1982.
7. Octave JN, Schneider YJ, Trouet A, Crichton RR: Trends Biochem Sci 8:217, 1983.
8. Trowbridge I: Biochem Pharm 1984.
9. Keen, JH, Maxfield, FR, Hardegree, MC Habid WH: Proc Natl Acad Sci USA 79:2912, 1982.
10. Olsnes S, Sanvig K: In Pastan I, Willingham M (eds): "Receptor-Mediated Endocytosis," New York: Plenum Press, 1984 (in press).
11. Helenius A, Marsh M, White J: J Gen Virol 58:47, 1982.
12. Van Leuven F, Cassiman JJ, Van den Berghe H: Cell 20:37, 1980.
13. Kaplan J: Cell 19:197, 1980.
14. Steer CJ, Ashwell G: J Biol Chem 255:3008, 1980.
15. Warren R, Doyle D: J Biol Chem 256:1346, 1981.
16. Basu SK, Goldstein JL, Anderson RGW, Brown MS: Cell 24:493, 1981.
17. Brown MS, Anderson RGW, Goldstein JL: Cell 32:6633, 1983.
18. Yamashiro DJ, Tycko B, Fluss SR, Maxfield FR: Cell 37:789, 1984.
19. Kaplan J. Nielsen MN: J Biol Chem 254:7329, 1979.
20. Van Leuven F, Cassiman JJ, Van de Berghe H: J Biol Chem 254:5155, 1979.
21. Karin M, Mintz B: J Biol Chem 256:3245, 1981.
22. Ciechanover A, Schwartz AL, Dautry-Varsat A, Lodish HF: J Biol Chem 258:9681, 1983.
23. Iacopetta BJ, Morgan EH: J Biol Chem 258:9108, 1983.
24. Klausner RD, Van Renswoude J, Ashwell G, Kempf C, Schecter AN, Dean A, Bridges KR: J Biol Chem 258:4715, 1983.
25. Maxfield FR: In Pastan I, Willingham M (eds): "Receptor-Mediated Endocytosis," New York: Plenum Press, 1984 (in press).
26. Heiple JM, Taylor DL: In "Intracellular pH: Its Measurement, Regulation, and Utilization in Cellular Functions," New York: Alan R. Liss, 1982, pp 22-54.
27. Tycko B, Keith CH, Maxfield FR: J Cell Biol 97:1762, 1983.
28. Anderson, RGW, Goldstein JL, Brown MS: Proc Natl Acad Sci USA 73:24234, 1976.
29. Pastan I, Willingham MC: Trends Biochem Sci 8:250, 1983.
30. Sandvig K, Olsnes S: J Cell Biol 87:828, 1980.
31. Draper RK, Simon MI: J Cell Biol 87:849, 1980.
32. Marsh M, Bolzau E, Helenius A: Cell 32:931, 1983.
33. Ohkuma S, Poole B: Proc Natl Acad Sci USA 75:3327, 1978.
34. Poole, B, Ohkuma S: J Cell Biol 90:665, 1981.
35. Maxfield FR: J Cell Biol 95:676, 1982.
36. Tietze CP, Schlessinger P, Stahl P: J Cell Biol 92:417, 1982.
37. Gonzales-Noriega A, Grubb JH, Talkad V, Sly WS: J Cell Biol 85:839, 1980.
38. Haigler HT, Maxfield FR, Willingham MC, Pastan I: J Biol Chem 255:1239, 1980.
39. Tycko B, Maxfield FR: Cell 28:643, 1982.
40. Harding C, Heuser J, Stahl P: J Cell Biol 97:329, 1983.
41. Iacopetta BJ, Morgan EH, Yeoh GCT: J Histochem Cytochem 31:336, 1983.
42. Willingham MC, Hanover JA, Dickson RD, Pastan I: Proc Natl Acad Sci USA 81:175, 1984.
43. Van Renswoude JK, Bridges KR, Harford JB, Klausner RD: Proc Natl Acad Sci US 79:6186, 1982.
44. Dickson RB, Hanover JA, Willingham ML, Pastan I: Biochemistry 22:5667, 1983.
45. Hemmaplardh D, Morgan EH: Br J Haematol 36:85, 1977.
46. Octave JN, Schneider YJ, Trouet A, Crichton RR: Eur J Biochem 115:611, 1981.
47. Willingham MC, Maxfield FR, Pastan I: J Cell Biol 82:614, 1979.
48. Dickson RB, Willingham MC, Pastan I: J Cell Biol 89:29, 1981.
49. Bleil JD, Bretscher MS: EMBO J 1:351, 1982.
50. Wall DA, Wilson G, Hubbard AL: Cell 21:79, 1980.
51. Geuze HJ, Slot JW, Strous GJAM, Schwartz AL: Eur J Cell Biol 32:38, 1983.
52. Hopkins CR: Cell 35:321, 1983.
53. Hopkins CR, Trowbridge IS: J Cell Biol 97:508, 1983.
54. Helenius A, Mellman I, Wall D, Hubbard A: Trends Biochem Sci 8:245, 1983.
55. Geuze HJ, Slot JW, Strous GJAM, Lodish HF, Schwartz AL: Cell 32:277, 1983.
56. Enns CA, Larrick JW, Suomalainen H, Schroeder J, Sussman HH: J Cell Biol 97:579, 1983.
57. Lamb JE, Ray F, Ward JH, Kushner JP, Kaplan J: Biol Chem 258:8751, 1983.
58. Friend DS, Farquhar MG: J Cell Biol 35:357, 1967.

59. Keen JH, Willingham MC, Pastan I: J Biol Chem 256:2538, 1981.
60. Willingham MC, Keen JH, Pastan IH: Exp Cell Res 132:329, 1981.
61. Virtanen I, Ekblom P, Laurila P: J Cell Biol 85:429, 1980.
62. Tartakoff AM, Vassalli P: J Cell Biol 97:1243, 1983.
63. Farquhar MG: Fed Proc 42:2407, 1983.
64. Oka JA, Weigel PH: J Biol Chem 258:10253, 1983.
65. Ohkuma S, Moriyama Y, Takano T: Proc Natl Acad Sci USA 79:2758, 1982.
66. Schneider DL: J Biol Chem 256:3858, 1981.
67. Schneider DL: J Biol Chem 258:1833, 1983.
68. Yamashiro DJ, Fluss SR, Maxfield FR: J Cell Biol 97:929, 1983.
69. Galloway CJ, Dean GE, Marsh M, Rudnick G, Mellman I: Proc Natl Acad Sci USA 80:3334, 1983.
70. Merion M, Schlesinger P, Brooks RM, Moehring JM, Moehring TJ, Sly WS: Proc Natl Acad Sci USA 80:5315, 1983.
71. Forgac M, Cantley L, Wiedenmann B, Altstiel L, Branton D: Proc Natl Acad Sci USA 80:1300, 1983.
72. Stone D, Xie XS, Racker E: J Biol Chem 258:4059, 1983.
73. Glickman J, Croen K, Kelly S, Al-Awqati Q: J Cell Biol 97:1303, 1983.
74. Cantley LC Jr, Cantley LG, Josephson L: J Biol Chem 253:7361, 1978.
75. O'Neal SG, Rhoades DB, Racker E: Biochem Biophys Res Commun 89:845, 1979.
76. Stekhoven FS, Bonting SL: Physiol Rev 61:1, 1981.
77. Stone DK, Xie XS, Racker E: J Biol Chem 259:2701, 1984.
78. Xie XS, Stone DK, Racker E: J Biol Chem 258:14834, 1983.
79. Gluck S, Cannon C, Al-Awqati Q: Proc Natl Acad Sci USA 79:4327, 1982.